THE PROPAGATION OF SOLAR FLARE PARTICLES IN A CORONAL LOOP

J. M. Ryan

Space Science Center
University of New Hampshire
Durham, New Hampshire 03824 USA

ABSTRACT

Energetic solar flare particles, both electrons and protons, must survive the turbulent environment of a flaring loop and propagate to the lower corona or chromosphere in order to produce hard x-ray and γ-ray bursts. This plasma turbulence, often observed in soft x-ray line widths to be in excess of 100 km/s, is presumably capable of efficiently scattering the fast flare particles. To some degree this prevents the free streaming of accelerated particles and, depending on the amplitude of the turbulence, restricts the particle transport to diffusive propagation along the length of the loop to the target chromosphere. In addition this turbulence is capable of performing additional acceleration on the fast particles by the second order Fermi mechanism. For compact flares with rise times < 2s, the acceleration effect is small and the propagation of the particles is governed by spatial diffusion and energy loss in the ambient medium.

A time-dependent diffusion equation with velocity-dependent diffusion and energy-loss coefficients has been solved for the case where energetic solar particles are injected into a coronal loop and then diffuse out the ends of the loop into the lower corona/chromosphere. The solution yields for the case of relativistic electrons, precipitation rates and populations which are necessary for calculating thick and thin target x-ray emission. It follows that the thick target emission is necessarily delayed with respect to the particle acceleration or injection by more than the mere travel time of the particle over the loop length. In addition the time-dependent electron population at the top of the loop is calculated. This is useful in estimating the resulting μ-wave emission. The results show relative timing differences in the different emission processes which are functions of particle species, energy and the point of injection of the particles into the loop. Equivalent quantities are calculated for non-relativistic protons.

1. Introduction

Short bursts of energetic solar radiation are frequently ascribed to energetic particles precipitating onto the lower corona or chromosphere after being accelerated higher in the corona. The duration or rise time of these bursts (x-rays or γ-rays) bears upon the acceleration time of the particles (electrons or protons/ions). However, the duration and rise time of the bursts of precipitating particles is also affected, sometimes greatly, by their propagation to these denser regions of the solar atmosphere.

Many of the papers presented in these volumes focus upon the nature of the brief or rapid fluctuations in x- or γ-ray emission from flares, and it is the aim of this paper to consider the effects of particle propagation on these observed rapid fluctuations. Without such a discussion incorrect conclusions about acceleration processes can be drawn from the time profiles of these bursts. One of the major findings of the SMM program is the discovery of a new time domain for bursts or spikes of hard x-rays and γ-rays. Bursts have been observed in x-rays on the order of tens of milliseconds (Kiplinger et al., 1983) while bursts of γ-rays have been as short as ∿ 1 second (Kane et al., 1985). These times are on the order of the travel times of electrons or protons over 2×10^4 km.

The propagation of electrons in a solar flare also affects the nature of μ-wave emission. The μ-wave opacity of a coronal loop or a flaring region is a strong function of electron density and thus altitude. The controversy as to whether μ-wave and x-ray emissions are results of the same electron population is further complicated by the fact that one initial population of electrons can spatially fractionate due to propagation effects which then leads to different signatures in x-rays and μ-waves due to the spatial dependence of the emission process.

A variety of scenarios exists for how particles once accelerated and injected into a coronal loop make their way to a region where they can emit observable radiation. The model chosen for study here is a simple one where particle propagation is separate and distinct from the acceleration process. Such a distinction is not clear for stochastic acceleration processes such as shocks and second order Fermi acceleration. In those cases, the propagation of particles is intimately linked to their acceleration. The problem of time scales in the related processes of stochastic acceleration and spatial diffusion is discussed by Schlickeiser (1985). In the environment of a solar flare where the spatial scale, magnetic field strength and ion density are 2×10^4 km, 100G and 10^9 cm^{-3} respectively, the product of the spatial diffusion time constant and the stochastic acceleration time constant is 80 s^2. Thus, if we restrict the discussion to the spatial diffusion time scale of 2 s, it implies that the acceleration time scale is 40 s making acceleration a minor feature in the propagation of particles within the loop. Thus, for these brief events the subsequent transport of particles after rapid acceleration involves negligible additional acceleration.

2. Model

We can analyze theoretically the transport of particles within a coronal loop after a rapid episode of acceleration, where the time domain of interest is under 2 seconds for the buildup or peaking of particle precipitation or the transport of electrons to optically thin regions of the corona. This model describing the particle transport and the rates of interest (e.g., precipitation rates, etc.) is a one-dimensional diffusion equation with an energy dependent diffusion coefficient and energy loss term.

To pose the basic problem simply, we assume that a coronal loop contains a uniform distribution of thermal material and is connected at both ends to the chromosphere. A distribution of particles is impulsively injected at an arbitrary point within the loop whereby the particles diffuse within the loop according to an energy dependent diffusion coefficient which is independent of time and space. The particles diffuse along the length of the loop away from the point of injection or acceleration. The diffusion process itself is one of elastic pitch angle scattering of the particles off an MHD wave field. We have assumed here no specific origin of the wave field, which could be anything ranging from an ambient wave field produced by photospheric turbulence to a wave field generated by the particles themselves.

In the process of diffusing, these energetic particles emit x-rays, γ-rays and μ-waves as the electrons and proton/ions interact with the ambient material and magnetic field inside the loop. When the electrons and/or protons reach the footpoints of the loop, they emit a burst of x-/γ-rays. Similarly, when the electrons reach an optically thin point in the loop, they emit observable μ-waves. The material inside the loop which is responsible for the initial thin target x-/γ-rays also serves to slow down the energetic particles through collisions with ambient thermal electrons. It is therefore necessary to follow the population of energetic particles in space, time and energy as they diffuse away from an assumed impulsive injection or acceleration. The case of finite duration injections can be handled by integrating the solution of the impulsive injection case over the injection time interval. If, however, the scattering wave field is due to the energetic particles themselves then the diffusion coefficient must also be time dependent. This complication is not addressed here.

The basic equation is the following

$$\frac{\partial f}{\partial t} - \frac{\partial}{\partial x}\kappa(E)\frac{\partial f}{\partial x} + \frac{\partial}{\partial E}\dot{E}(E)f = Q \qquad (1)$$

where f = distribution function of particles,
x = distance along loop,
κ = diffusion coefficient,
E = energy of particle,
$\dot{E}$ = energy loss rate for collisional deceleration and
Q = injection profile.

We take $Q = \delta(x - x')\delta(t)S(E)$ where S is the input particle distribution and then (1) can be solved with the boundary conditions $f = 0$ at $x = 0,\ell$, where ℓ is the total loop length. Using a Laplace transformation in time and by expanding in eigenfunctions in x (1) yields

$$f(x,x';E,t) = \sum_m \frac{2}{\ell}\sin\frac{m\pi x'}{\ell}\sin\frac{m\pi x}{\ell}\exp(-\eta_m(E,E'))S(E'). \qquad (2)$$

Here E' is determined by the slow down relationship

$$t + \int_{E}^{E'} \frac{d\varepsilon}{\dot{E}(\varepsilon)} = 0 \tag{3}$$

and

$$\eta_m(E, E') = \int_{E}^{E'} \frac{-\frac{\partial \dot{E}}{\partial \varepsilon} - \kappa(\varepsilon) \frac{m^2\pi^2}{\ell^2}}{\dot{E}} d\varepsilon. \tag{4}$$

The quantity E' is thus the particle energy projected backward in time to t = 0. Integrating over x space, the total loop population is

$$f(E,t) = \frac{4}{\pi} S(E') \sum_{m=1,3,5,\ldots} \frac{1}{m} \sin\frac{m\pi x'}{\ell} \exp(-\eta_m(E,E')) \tag{5}$$

The total flux of particles diffusing out the ends of the loop is the quantity

$$\dot{f}(E,t) = \kappa(E) \left(\nabla f(x=0,E) - \nabla f(x=\ell,E)\right) \tag{6}$$

which is

$$= \frac{4\pi}{\ell^2} \kappa(E) S(E') \sum_{m=1,3,5,\ldots} m \sin\frac{m\pi x'}{\ell} \exp(-\eta_m(E,E')). \tag{7}$$

Other quantities of interest can be calculated similarly.

Two cases of interest can be investigated, that of (1) relativistic electrons where the energy loss is constant (as is the diffusion coefficient) and (2) $\sim$ 20 MeV protons which are sub-relativistic ($\kappa \sim E^{+\frac{1}{2}}$ and $\dot{E} \sim E^{-2}$). The energy dependence of κ is only due to velocity differences, i.e. the mean free path of the particle is taken to be constant. As will be seen, the results are similar so that the relativistic electron calculation can be taken to be representative of the basic physics.

X-rays and γ-rays can be emitted by electrons and protons, respectively, from both the regions of precipitation at the ends of the loop and from the interior of the loop where tenuous thermal material resides; μ-waves on the other hand might very well only be emitted from the highest parts of the loop which are presumably optically thin. Appropriate time profiles for such emissions can be derived by calculating the population or population flux of

the parent particles for various injection positions and material densities within the loop.

Figure 1 is a plot of total particle precipitation rate with an input spectrum of $E^{-2.5}$ at t = 0. These profiles would be identified with total instantaneous thick targe x-/γ-ray emissions. Here particles are injected at the midpoint of the loop ($x/\ell = \frac{1}{2}$) and at $x/\ell = \frac{1}{4}$ and 1/10. The time axis is normalized to the characteristic diffusion time of the particles $\tau_d = (\kappa(E)/\pi^2\ell^2)^{-1}$ and the density effect is included as a parameter τ_d/τ_c where $\tau_c = E/\dot{E}$. The vertical axis, i.e. precipitation rate, is in units of τ_d normalized to the total injection population. Values of τ_d/τ_c are 0, 1 and 5 which represent respectively, the case with no material inside the loop, the case with a quantity of material such that energy loss competes with diffusive losses and the case where energy losses dominate.

Curves with equal τ_d/τ_c show that the peak precipitation rate is solely a function of injection position but the actual time of peaking is weakly dependent on the ambient density. The density effect is mostly seen in the amplitude of the precipitation in the latter half of the pulse. The earlier peaking of the curves for smaller x'/ℓ show that particles diffuse preferentially out the closest end of the loop, the distance to which is strongly related to peak time. In terms of the dimensionless quantities τ_d/τ_c, there is little difference between the curves for relativistic electrons and subrelativistic protons.

Figure 2 is a similar plot where the precipitation rate for each loop end is shown separately. This sort of time profile would be expected from observations by an instrument which could spatially resolve two emission points. The density effects here are seen as a variation in the amplitude of the precipitation rate at the far end of the loop. The relative peaking times again are only a function of position. The loop end closest to the injection position shows the greatest precipitation and the closer the injection point is to the end, the earlier the peak in the precipitation rate. The peak time of the precipitation out the farthest loop end is not sensitive to the injection position as the particles must diffuse rather uniformly through the loop to produce any significant precipitation at the remote site. This time is roughly the same for all cases, i.e., τ_d.

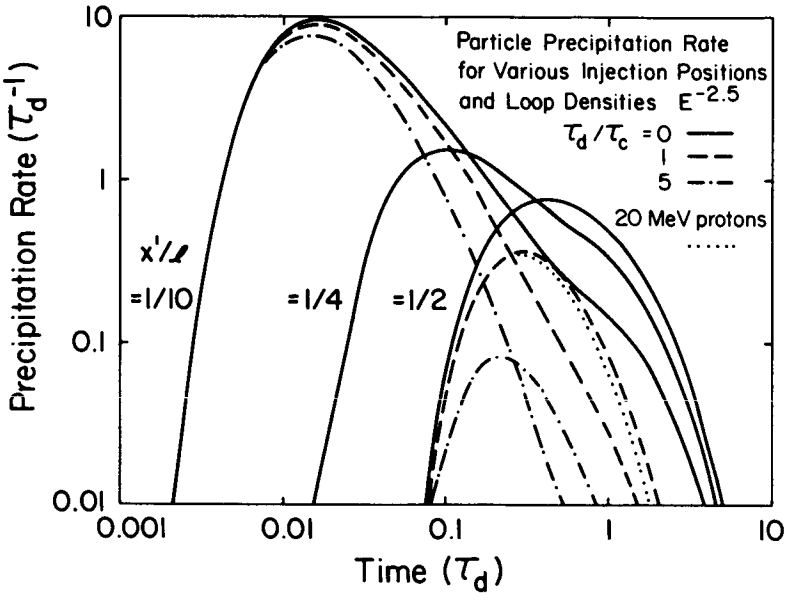

Figure 1. Total particle precipitation rate versus time for various injection positions and loop densities, where the time axis is in units of the characteristic diffusion time. The precipitation rate is in dimensionless units of inverse diffusion time, and the loop densities are parameterized by τ_c the collisional slow-down time and then normalized to the characteristic diffusion time. An injection position of $x'/\ell = 1/10$ means that energetic particles in this case with a spectrum of $E^{-2.5}$ are injected at one tenth the way from one end of the loop to the other. Also shown are the corresponding curves for 20 MeV protons which have a different energy dependence for collisional braking.

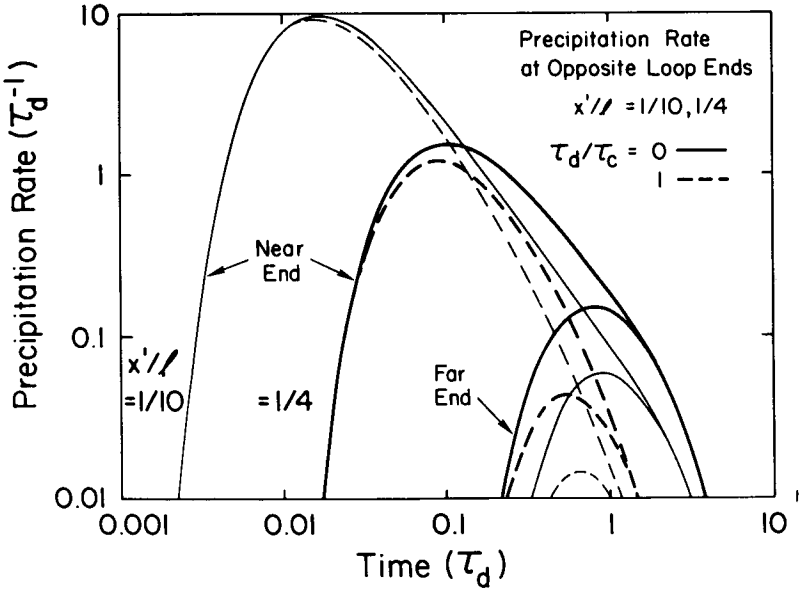

Figure 2. The particle precipitation rate for opposite ends of the loop for injection positions of 1/10 and 1/4. Curves are shown for the precipitation

rate at the loop end nearest the injection point and the loop end farthest from the injection. There is almost two orders of magnitude difference between the rates at opposite ends of the loop when particles are injected very close to one end. Collisional braking further suppresses the rate at the far end due to the greater time required to diffuse to the far end.

We expect that x- and γ-ray emission comes not only from the footpoints of the loop, but also from the interior of the loop due to the non-zero matter density. This thin target emission will be proportional to the number of particles still within the loop. In Figure 3 is the total loop population as a function of time plotted along with the precipitation rate illustrating the relative rates of thin versus thick target emission. These are plotted for the case where $x'/\ell = \frac{1}{4}$ and $\tau_d/\tau_c = 1$. Also shown is the ratio of these two quantities. It should be noted again that the emission physics is not included in these calculations but the total emission will scale by the quantities shown. The ratio of loop population to precipitation reaches a constant value as time approaches τ_d. At this time particles have uniformly distributed themselves throughout the loop and from that time forward the precipitation rate is simply proportional to the loop population. The positional dependency at t = 0 has been lost.

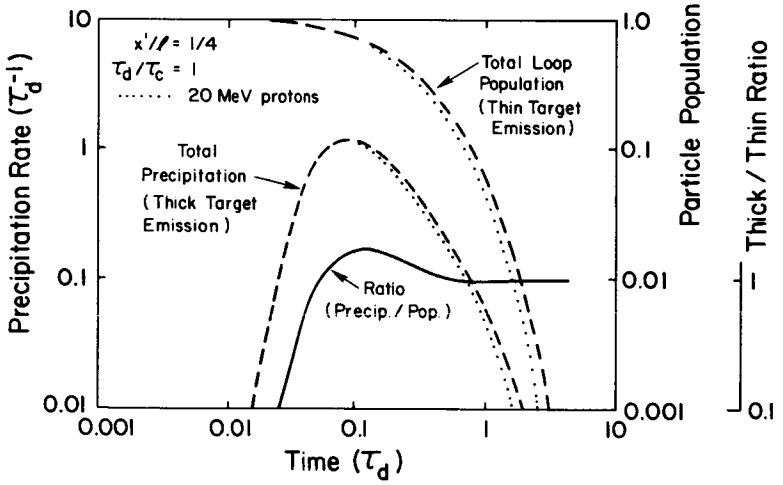

Figure 3. Total precipitation rate representative of thick target emission processes and the time behavior of the total particle population representative of thin target emission processes. The ratio of the two quantities is also shown where thin target emission dominates at the very earliest times due to the fact that no particles have diffused to the ends of the loop. Also shown are equivalent curves for the 20 MeV protons.

Figure 3 has other relevancy if the whole contents of the loop is optically thin to μ-waves. In this case the thin target emission and the μ-wave emission will follow the total loop population. The total loop population, of

course, peaks at t = 0 as would the μ-wave emission in this case. The precipitation produced x-rays peak at a later time, a function of x'/ℓ.

If the case exists, however, that only part of the loop is optically thin to μ-waves, specifically the top quarter of the loop, then the emission will follow the particle population in that top quarter of the loop. This is shown in Figure 4 again with the accompanying precipitation profile for the case of x'/ℓ = 1/10 and for a few values of τ_d/τ_c. In this configuration the x-ray flux (precipitation) will lead the μ-wave flux (population) since the injection point is closer to the loop end than to the top of the loop.

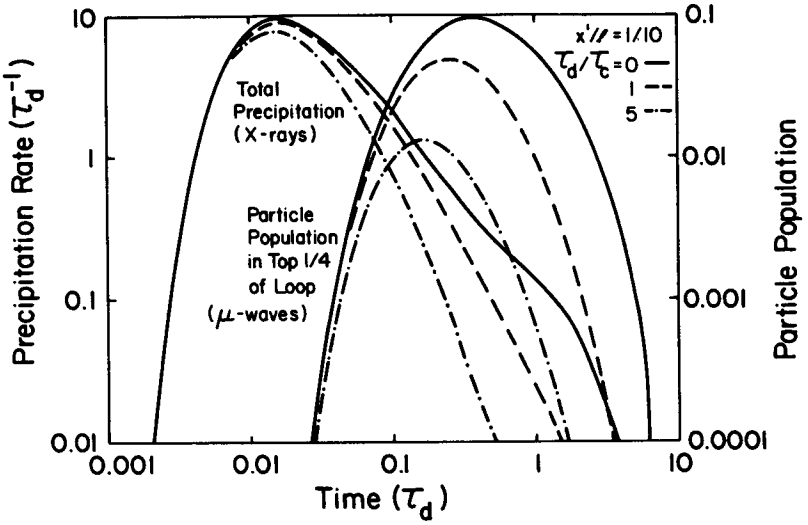

Figure 4. Total precipitation rate representing hard x-ray emission and the time behavior of the electron population representing μ-wave emissions at the very top 1/4 of the loop (presumed to be optically thin). The material density inside the loop has little impact on the relative timing of the two emissions.

Parameterizing all these curves in terms of τ_d and τ_c is a useful exercise even though we expect significantly different profiles from subrelativistic protons as opposed to relativistic electrons. But in terms of these quantities the profiles are very similar as seen in Figures 1 and 3. Thus the energy dependences of any of these profiles are imbedded in the scaling of the axes. A different profile, though, is to be expected if κ exhibits an abrupt change of form. This would occur for mildly relativistic electrons as they interact with whistlers at lower energies and MHD waves at higher energies.

3. Discussion

Since second order stochastic acceleration occurs due to the same scattering or diffusion process, it is possible that acceleration is not negligible compared to spatial diffusion effects. However, this is true only when

the mean-free path is very short compared to loop length in which case the particles are accelerated efficiently but do not propagate beyond the acceleration region. If in fact, the turbulence in the flaring loop is not associated with the acceleration of the energetic particles, the particle transport is truly decoupled from the acceleration. In this scenario episodic acceleration could occur in one region of the loop and then the particles which escape this region into the remainder of the loop are the ones described by the above formalism. The turbulence necessary for the diffusion approximation to be valid could then come from three potential sources, photospheric turbulence propagating upward and cascading to larger κ values, flare generated waves or waves excited specifically by the fast particles. Particle excited waves would allow for scatter-free propagation of electrons prior to the development of a sufficient intensity wave field to isotropize the distribution. Thus it would be possible to achieve the very short time scale phenomena observed by Kiplinger et al. (1983), yet the majority of the particles would obey diffusive transport once the wave field develops. This is consistent with the observations of Kiplinger et al., (1983) as these short (< 50 ms) bursts of x-rays are infrequent occurrences with an energy content far less than the total x-ray flux. The majority of hard x-rays and γ-rays reside within a time envelope which has a longer time scale than that of the very shortest spikes. These could be photons from a majority of particles which obey diffusive propagation while the infrequent but rapid spikes derive from particles (electrons) which freely propagate to the loop footpoints before a sufficient scattering wave field develops.

The concept of diffusive transport of energetic particles within a flaring coronal loop is an attractive one in that we assume that the flare environment is turbulent and noisy, a likely situation. This contrasts with precipitation models based on simple strong pitch angle diffusion at a single point while the remainder of the loop is quiet, e.g. (Zweibel and Haber, 1983; Kawamura et al., 1981). It is unfortunately difficult to verify the existence of the MHD wave field necessary for pitch angle scattering over such a large spatial extent. Large scale turbulence (> 100 km/s) is commonly seen in broad soft x-ray lines but this normally takes place very early in the event. If the wave field is generated by the fast particles, only a small fraction of the particle energy density is required in a small range of wave number resonant with the particles. This may be entirely unobservable. However, this can be observed in situ at the Earth's bow shock (Lee, 1982) where fast ions generate the waves necessary for their own acceleration in the environment of that shock.

In summary, the physics of short time scale phenomena must take into account the effects of particle transport between the times of particle acceleration and production of observable radiation. Diffusive particle propagation effects are capable of producing a number of timing features seen in solar flares by varying geometrical parameters such as the length of the loop, the relative position of the particle injection and the position of the portion of the loop optically thin to μ-waves. If such a transport concept is

used as a working model in hard x-ray, μ-wave and γ-ray emission, then the time profile of these emission processes become diagnostic tools in probing the interior of flaring coronal loops.

4. References

Kane, S. R., Chupp, E. L., Forrest, D. J., Share G. H., and Rieger, E. 1986, Vol. 2, these proceedings.

Kawamura, K., Omukoda, T., and Suzuki, I. 1981, Solar Phys., 11, 55.

Kiplinger, A. L., Dennis, B. R., Emslie, A. G., Frost, K. J., and Orwig, L. E. 1983, Ap. J. (Lett.) 265, L99.

Lee, M. A. 1982, J. Geophys. Res., 87, 5063.

Schlickeiser, R. 1985, Proc. 4th Intl. Summer School on Cosmic Ray Astrophys., ed. M.M. Shapiro, (Dordrecht: D. Reidel) in press.

Zweibel, E., and Haber, D 1983, Ap. J., 264, 642.